Effect of Hydrodynamically Designed Blades on the Efficiency of a Michell-Banki Turbine

Jorge Sierra Del Rio**‡, Steven Galvis-Holguin***, Diego Hincapié-Zuluaga****, Chica E. *****

*Department of Mechatronics Engineering, Instituto Tecnológico Metropolitano, Professor, 050034.

**Department of Engineering, Environmental Research Group – GIIAM, Institución Universitaria Pascual Bravo, 050034.

*** Department of Mechatronics Engineering, Instituto Tecnológico Metropolitano, Former Student, 050034.

**** Department of Mechatronics Engineering, Instituto Tecnológico Metropolitano, Professor, 050034.

***** Department of Mechanics Engineering, Universidad De Antioquia, Professor, 050034.

(jorgesierra@itm.edu.co, stevengalvis221631@correo.itm.edu.co, diegohincapie@itm.edu.co, edwin.chica@udea.edu.co)

‡
Corresponding Author; Jorge Sierra Del Rio, 050034, Tel: +57 301 357 4232, jorgesierra@itm.edu.co

Abstract- The small hydroelectric power plants –SHPP's- are implemented in non-interconnected zones –NIZ- of developing countries. In which, the provision of electrical energy from the national interconnected system is not economically feasible. Therefore, Michell-Banki turbines could be installed, which, despite having lower efficiencies than turbines such as Pelton and Francis, maintain their efficiency although fluctuations in site conditions. For this reason, different studies have been made to increase the efficiency of the Michell-Banki turbine by making geometric modifications to both the nozzle and the runner. However, few studies have been carried out with respect to the incidence of the profile of the rotor blades on the efficiency of the turbine. This work presents a numerical study conducted in ANSYS CFX® V18.1 that seeks to improve the efficiency of a Michell-Banki turbine by modifying one of its geometric parameters: the profile of the blades in the runner. Four aerodynamic profiles, 20-32C, A18, NACA 9412-15 and NACA 9412-ST, were selected and modified. Subsequently, they were integrated into the turbine runner to compare their performance to that of a turbine model configured with the conventional blade profile by means of computer simulations. In total, five (5) turbine models were studied under the same operating conditions: inlet flow velocity, 3.6 m/s; runner angular velocity, 450 RPM; and outlet pressure, 1 atm. The simulation results revealed an efficiency increase regarding the model configured with conventional profiles of 7.37%, 7% and 0.76% with 20-32C, NACA 9412-ST and NACA 9412-15 blade profiles, respectively.

Keywords ANSYS CFX; Cross-flow turbine; Hydrodynamic profile; CFD analysis; Micropower; Transient simulation.

1. Introduction

In the past three decades, the planet has been experiencing the consequences of climate change due to the high greenhouse-effect gases (GEG) and the excessive use of fossil fuels, [1]. Due to this and the growing demand of energy, the scientific community has been forced to look for alternative sources of electric power generation [[2], such as wind, solar, hydroelectric and geothermal [3]; where the hydroelectric energy is the most important in recent decades [4].

The costs associated with generation, transmission and distribution of electricity have made that the provision of electric service in the NIZ (non-interconnected zones) of the developing countries is mainly performed by means of diesel generation plants, solar panels and small hydro power plants [5]. Among the renewable energy resources, micro-Hydropower systems are a solution for stand-alone/residential electric generation in small communities non-interconnected to national electric grid. Also, achieving energy security and reducing poverty in the NIZ.

The implementation of small hydraulic turbines, specially Michell-Banki type, enables to supply electrical energy to such NIZ and provide them with a better quality of life, with low maintenance and installation costs for the turbomachinery. This type of turbine is used in micro hydro power systems due to its simple structure, easy to manufacture and presents a consistent performance during flow rate (Q) variations [6]. Similar to other types of turbines, such as Kaplan, Pelton and Francis, this is a mechanical system characterized by the continuous rotation of a runner caused by

a fluid (water) and the conversion of the mechanical power in such rotation into electrical energy by means of a generator. Michell-Banki turbines have a typical efficiency in the range of 70-85%. According to OSSBERGER®, a manufacturer of a Michell-Banki type turbine, it is designed for power ranges between 15kW and 5000kW and can be adapted to variable flow rates [7].

Such turbine is comprised of a runner, nozzle, guide vane, casing and the runner, as shown in Fig. 1. Its operation starts with the entry of water through the nozzle, which regulates the water flow with the guide vane position. The main function of the nozzle is to accelerate and guide the water at the correct angle with respect to the runner. Besides, it distributes the fluid in an even manner so that the stress caused by the velocity of the fluid is transferred to the entire surface of the blade. The runner is the most important body in the turbine because it is responsible for converting the kinetic energy in the fluid into mechanical rotational energy. Such conversion is caused by the drag of the water jet that hits the blades, which is proportional to the water velocity; therefore, the stronger the drag, the higher the tangential velocity of the runner [8]].
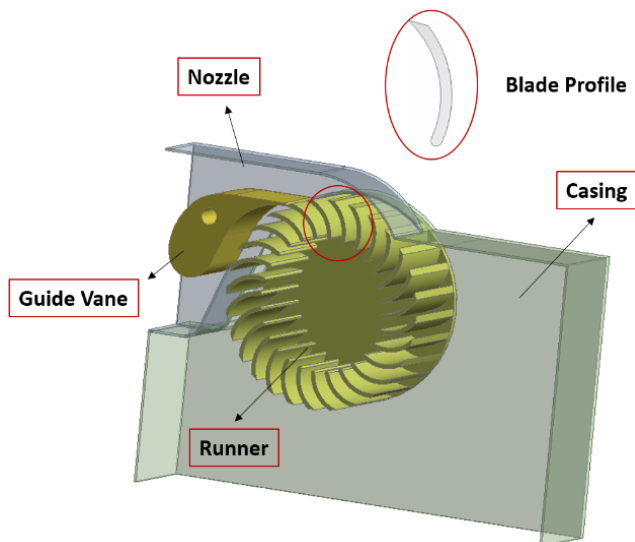

Fig. 1. Configuration of a Michell-Banki turbine.

The energy transfer occurs in two stages, as shown in Fig. 2. Stage 1 takes place when water enters the runner and 70% of the energy is transferred to it. During Stage 2, the water leaves the runner and transfers the remaining 30%. Because of this flow phenomenon, Michelle-Banki turbine is considered a two-stage partial impulse turbine. Since the first stage works with a reaction degree under the pure impulse principle [9].
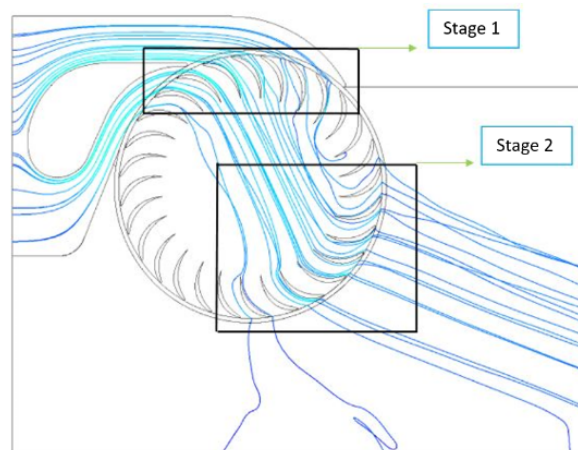

Fig. 2. Energy transfer stages in a Michell-Banki turbine.

The literature includes different numerical and experimental studies establishing the influence of geometric parameters on the efficiency of a Michell-Banki turbine. Based on experimental studies, several authors have conducted numerical studies based on CFD techniques and determined the incidence of geometric and operating parameters on the efficiency of a Michell Banki turbine. L. Velásquez and W. Enriquez (2012) investigated the influence of the guide vane angle on the hydraulic power of that type of turbine by means of computer simulations in ANSYS CFX®, they found that the optimal guide vane angle varies as a function of turbine size: 14.3° for the model and 15.3° for the prototype [10]. V. Sammartano, et al. (2013) developed a stationary state CFD simulation of three runner designs in a Michell-Banki turbine configured with 30, 35 and 40 sharp blades; they determined that an increase in the number of blades in the runner enhances its performance, the highest turbine efficiency was obtained with 35 blades. Nevertheless, they maintain that more than that number of blades represents a considerable restriction to the water flow, which causes the runner to generate less power [11]. In addition, C.S. Kaunda, et al. (2014), carried out a numerical study in ANSYS CFX® that delved into the flow profile of the same kind of turbine at the best efficiency point, the numerical results of the study were successfully compared to experimental results and it was observed that the best efficiency point is reached when the axis of the runner does not obstruct the flow profile. This assertion allows us to conclude that preventing the jet from colliding with the axis is important for designing cross-flow turbines [12]. Later, Y. L. Castañeda et al. (2017), conducted a numerical study in ANSYS CFX® on the incidence of the number of blades on the efficiency of a Michell-Banki turbine, such research implemented 6 turbine models, each with 16, 20, 23, 25, 28 and 32 blades, respectively. Based on the simulation results, the authors concluded that the efficiency of the turbine rises by 3.2% when the number of blades is increased from 16 to 28 [13].

As far as numerical investigations related to the blades geometry, M. A. Arellano (2015) developed a computer simulation with ANSYS CFX® that determined the incidence of the geometry of the rotor blades on the generated power. For that study, sharp and rounded blades of 2 different thicknesses were used. In total, 4 different runner models were

configured for constant operating conditions and the results of the numerical simulation validated the hypothesis of the author. It was observed that the turbine model configured with sharp blade profiles significantly influenced torque production by the runner; as a result, turbine efficiency was improved [14]. It is important to highlight that, despite the efficiency increase produced by enhancements in the sharp profile, such blades lose their sharpness more quickly due to abrasive wear (in comparison to the conventional blade profile), which noticeably reduces turbine efficiency in the short term. Moreover, Deny Adanta et al. conducted a research to verify the Michell-Banki turbine performance when operating with hydrodynamic profiles. To this end, 3 rotors were configured, variating only the blades geometry, and using NACA 6509 and 6712 profiles, which were compared to a model with conventional blades. This study showed efficiencies of 47.6%, 46.9% and 77.8% respectively. These low efficiencies may be due to the fact that the researches neither considered nor adjusted the radius and the curvature angle of the hydrodynamic profiles against the model with conventional blades.

This literature review shows that the hydrodynamic profile of the blade plays an important role in the efficiency of this type of turbine; however, there are not enough studies that link the former with the latter. The aim of this study is to determine, by computer simulations, the incidence of the hydrodynamic profile of the runner blades on the efficiency of a Michell-Banki turbine, Adjusting the geometry according to the curvature and length of the rope in the design with conventional profiles.
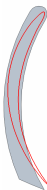
2. Method

2.1. Design method

The general purpose of theses numerical flow analysis through Michell-Banki turbine was to determine the fields of pressure and velocity and the incidence of the hydrodynamic profile of the runner blades on the efficiency of the turbine. The analysis was conducted on three dimensional models in the whole volume of flow, from the inlet stub pipe to the outflow part of the turbine. Therefore, 5 runner models were constructed: a standard runner with a conventional blade configuration and four runners fitted with blades with different hydrodynamic profiles modified (A18, 20-32C, NACA 9412-ST and NACA 9412-15). Which were selected by a criterion of dimensional similarity and then were their curvature modified according to the curvature of the conventional profiles. Table 1 presents the features of the profiles characterized by Chord Length factor, which is determined by the variation of the chord length of the reference profile compared to the modified profile.

Table 1. Characteristics of the hydrodynamic profiles of the blades.

Type of profile	Standard profile	Modified profile	Overlay	CL [%]
Conventio-nal		--	--	--
A18				7.2
20-32C				8.06
NACA9412-15				7.84
NACA9412-ST				6.9

The geometry of the main parts that compose the turbine is based on empirical correlations by OLADE [15]. This international organization presented a complete design procedure of cross-flow turbine. After each turbine with its casing was modelled using Autodesk Inventor, the control volume was extracted by means of Boolean subtractions. For configuration purposes, the domain between the runner, the casing and the nozzle was partitioned by including a volume ring, as shown in Fig. 3. Such ring simplifies the configuration of the interfaces between rotating and static bodies by setting the boundary conditions of each model.
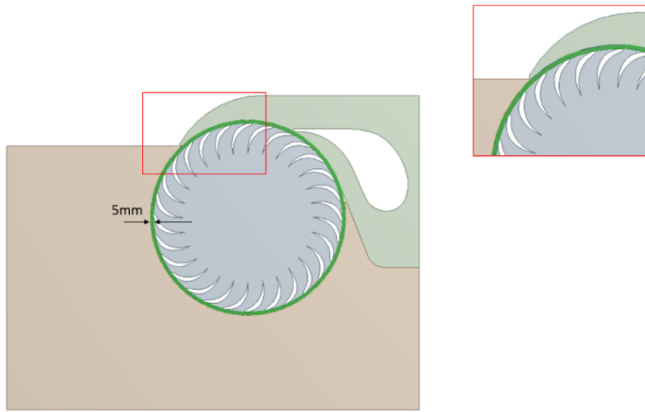
Fig. 3. Volume ring of the fluid inside the Michell Banki turbine.

Fig. 4 presents the mesh independence study obtained from the turbine model configured with the 20-32C profile according to the operational conditions of the turbine described in the boundary conditions specifications. The discretization process was completed with the Meshing module of the commercial software ANSYS Workbench V18.1®. Tetrahedral elements were implemented to create the control volume, thus achieving mesh independence with 17e6 elements. Also, variations under 2% were detected in the torque generated by the runner configured with the 20-32C profile, which was taken as reference. The characteristics identified in the mesh were maximum obliquity (0.82), maximum aspect ratio (9.53), minimum orthogonal quality (0.17) and minimum element quality (0.18).
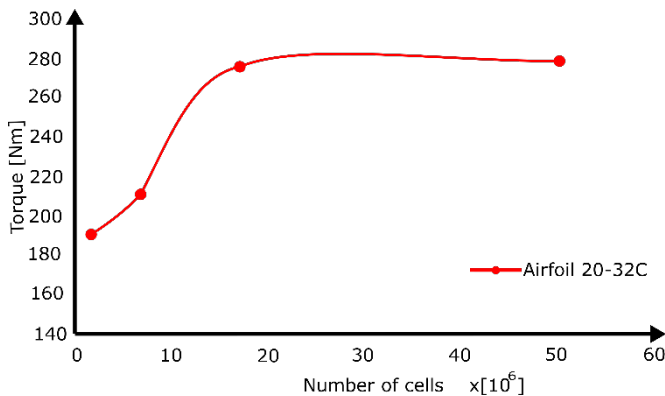

Fig. 4. Mesh independence study of the turbine model configured with the 20-32C profile.

Fig. 5 outlines the configuration of the boundary conditions. They are associated to the operating conditions of the turbine: angular velocity, 450RPM; net head, 10m; and volume flow rate, 0.148 m³/s. The boundary conditions that were used correspond to the operating conditions of the turbine. The fluid velocity is set in the injector entry at 3.2.m/s, which meets the site requirements conditions (Q and H) implemented in the investigation. As the simulation corresponds to a closed pipes system, the inlet pressure will depend on the height differential from the drop point of the flow to the rotor shaft. The outlet of the turbine is configured as an opening of "0" Pa manometric pressure, which enables the fluid to enter and exit the control volume. The walls of each domain were assumed to be non-slip. For the

configuration of the turbine runner, walls with angular velocity of 450 RPM with respect to the runner axis were considered. In order to transfer information between the rotational domain (runner) and the static bodies (casing and nozzle), the interface conditions among all the bodies were set as shown in Fig. 6. In total, two interfaces were configured. The first one corresponds to the surface between the ring, the nozzle and the casing, declared as fluid-fluid-type; this interface model is configured to be "general connection", as shown in Fig. 6a. Besides, Fig. 6b presents Interface 2, associated with the ring and the turbine runner (rotating domain). Similarly, the second interface is declared to be fluid-fluid-type and its interface model is "general connection" again. However, unlike Interface 1, in the Interface 2 the Frame change/mixing model is adjusted as transient rotor-stator; this ensures the transience of the physical magnitudes involved in the calculation when geometry variations occur due to the rotation of the domain.
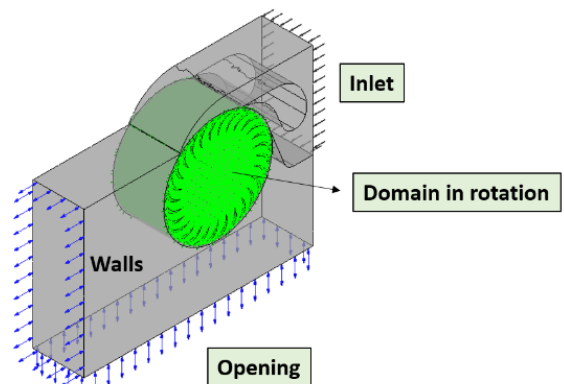
Fig. 5. Boundary condition configuration.
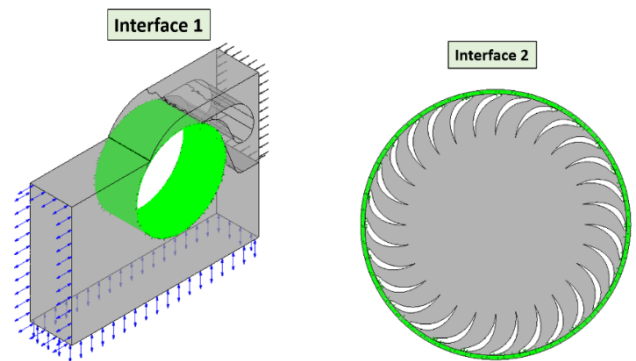
a. Interface between the ring, casing and nozzle.　**b.** Ring-runner interface.

Fig. 6. Configuration of interfaces between the nozzle, the casing and the runner of the Michell Banki turbine.

2.2. Numerical method

The process to solve mass and momentum conservation was conducted in the CFX module of ANSYS Workbench 18.1®. In order to obtain a reliable solution to the problem, the Roe-FD flow-type minimal implicit solution method was adopted along with a second-order spatial discretization of the equations, which ensure the quality of the mesh and the reduction of the error by discretization. The *k-ε* standard

turbulence model [16], was implemented by a transient simulation with time steps of 0.001 seconds. Furthermore, the total simulation time necessary to ensure stability in the response of the generated torque was 0.14 seconds. Therefore, the residuals under 1e-4 obtained by the Root Mean Square (RMS) and the stability in torque measurement at each timestep were the criteria to determine the convergence of the numerical study. The work fluid was biphasic, composed of water and air, and both fluids were under a subsonic flow regime (Ma<1), reference pressure of 1 atm y and 25°C. Additionally, the surface tension coefficient of the interface between the two fluids was set to 73.5 dynes/cm.

The initial conditions of the system are presented in Fig. 7. Red and blue indicate a water volume fraction of 1 and 0, respectively. The volume fraction of the nozzle is set to 1, with an initial speed of 3.6 m/s normal to the nozzle outlet. In the runner and casing, a water volume fraction of 0 was configured.
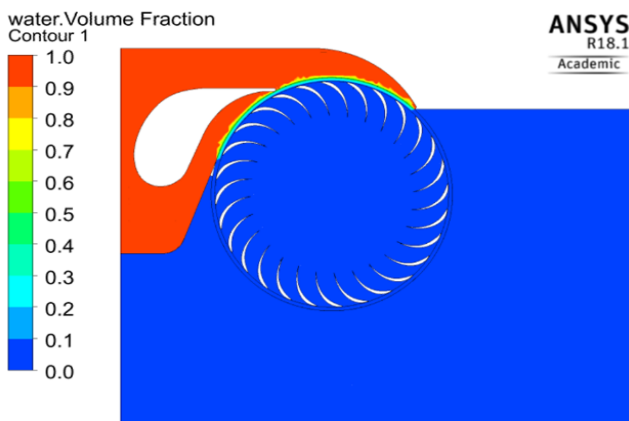

Fig. 7. Initial volume fraction conditions of the simulation.

The k-ε turbulence model introduces two new variables in the system of equations. The continuity equation is defined by (1):

$$\frac{\partial \rho Ui}{\partial t} + \frac{\partial}{\partial x_i}(\rho U_i) = 0 \tag{1}$$

The momentum equation is given by:

$$\frac{\partial \rho Ui}{\partial t} + \frac{\partial}{\partial x_i}(\rho U_i U_j) = -\frac{\partial p'}{\partial x_i} + \frac{\partial}{\partial x_j}\left[\mu_{eff}\left(\frac{\partial U_i}{\partial x_j} + \frac{\partial U_j}{\partial x_i}\right)\right] + S_M \tag{2}$$

Where 'S_M' is the sum of the forces of the bodies; 'μ_{eff}', effective viscosity caused by turbulence; and 'ρ', modified pressure.

The torque generated by the Michell Banki turbine was calculated by Equation (3), where 'S' refers to surfaces that include rotating domains; '$\hat{n}$', a unit vector normal to surface; '$\vec{r}$', the position vector; '$\hat{a}$', a unit vector parallel to the rotation axis; and '$\overline{\overline{\tau}}$', (total stress tensor) uses continuum mechanics to model stress at a point within the material [17].

$$T = \left[\int_S \left(\vec{r} \times (\overline{\overline{\tau}} \cdot \hat{n})\right) dS\right] \cdot \hat{a} \tag{3}$$

Assuming Zero pressure at the impeller outlet, Mockmore and Merryfield [18] defined the hydraulic efficiency of the machine (η) as the ration between the outlet power ($P_{out} = T \cdot \omega$) and the input power ($P_{in} = \gamma \cdot Q \cdot H \cdot \eta$) related to the hydraulic head in H at the inlet of the turbine and for a given water discharge Q, see equation (4).

$$\eta = \frac{T \cdot \omega}{\gamma \cdot Q \cdot H} \tag{4}$$

Where 'T' is the torque generated at the turbine runner and 'γ' is the specific weight of water ($\gamma = \rho \cdot g$). Beside ω, Q and H are the operating conditions of the turbine.

3. Results and Discussion

Table 2 shows the results of the most relevant dimensions of the Michell-Banki turbine design, for the five models studied, using the methodology given by OLADE [15].

Table 1. Geometrical configuration of the Michell-Banki turbine.

Design Parameter	Value
External diameter (D_{ext})	400 mm
Internal diameter (D_{in})	272 mm
Blade output angle (β_{2b})	90 °
Blade input angle ((β_{1b})	36 °
Number of blades	28
Runner width (W)	350 mm
Nozzle width (B)	130 mm
Nozzle height (h_0)	320 mm
Nozzle output arc (θ_s)	120 °

Fig. 8 presents the torque variation of the turbine as a function of time with the 5 different runner blade profiles. It can be seen that the torque stabilizes after 0.04 s (3 rotations) with all configurations, which allows us to conclude that a simulation time of 0.14 s (10.5 rotations) ensures a quasi-stationary behavior of the turbine, thus allowing to obtain the final generated torque.
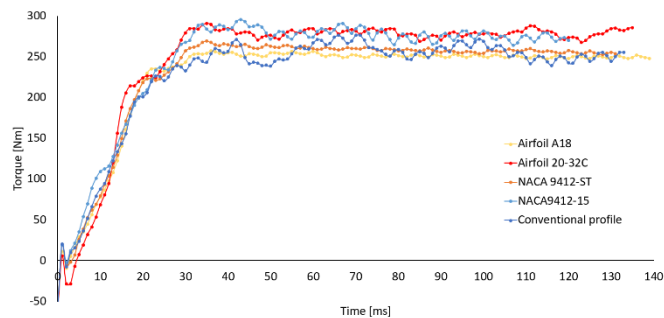
Fig. 8. Plot of generated torque with different turbine models.

Table 3 lists the average torque generated with each turbine configuration. The values are obtained by averaging the set of transient results and calculated only after the torque presents a quasi-stationary behavior. Besides, the efficiency of the turbine was determined by Equation (4). As a result, the maximum reported efficiency was 90.6% with the runner fitted with Airfoil 20-32C, which represents an increase in efficiency (7.37%) compared to the conventional blade turbine. The turbine configured with NACA 9412-15 blades presented the same efficiency, but a greater standard deviation.

Table 3. Torque generated by turbines with different runner configurations.

Blade profile	Generated torque [Nm]	Standard deviation	Efficiency by Eqn. (4)	Efficiency variation compared to conventional profile [%]
20-32C	278.91	4.43	90.6	7.37
NACA 9412-15	277.77	7.01	90.3	7
NACA 9412-ST	258.56	3.03	84.1	0.76
Conventional	256.23	9.79	83.3	--
A18	251.04	2.03	81.6	-2.15%

Fig. 9 presents the water-air volume fraction contours and the streamlines (characterized by velocity) of each model in the median plane of symmetry of the turbines. It can be seen that the runners of the turbines configured with profiles 20-32C and NACA 9412-15 tend to rotate more due to the flow profile exhibited by the water at the runner outlet, which is in line with the momentum theory. The latter holds that the

tangential component of the exit velocity of the fluid in the second stage applies a favorable rotation to the turbine, this leads to conclude that additional torque is generated by the momentum in these two models and not in the other cases.
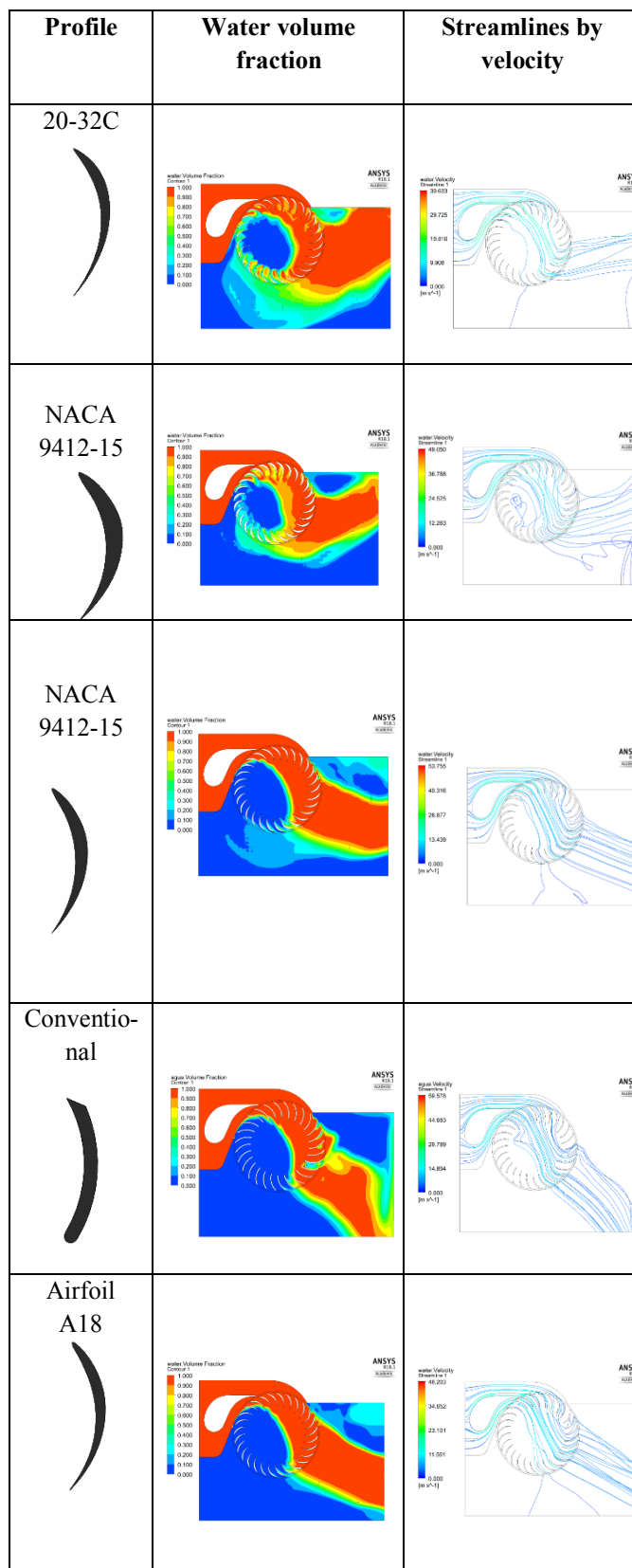
Profile	Water volume fraction	Streamlines by velocity
20-32C		
NACA 9412-15		
NACA 9412-15		
Conventional		
Airfoil A18		

Fig. 9. Contour of the water-air volume fraction and streamlines characterized by velocity in the median plane of symmetry of different turbine models.

The behavior of a turbomachine is described by the Euler equation (5), which expresses the effects of the interaction between the turbine and the fluid circulating through it. In order to explain this behavior, the velocity triangle in Fig. 10 is used, where 'U' is the tangential velocity of the blade; 'v', the velocity of the fluid; 'W', the relative velocity of the fluid, 'α', the flow angle; and 'β', the angle measured between the blade velocity and the relative velocity of the fluid.

$$P = \rho.Q.[(\overrightarrow{C_1}.\overrightarrow{U_1} - \overrightarrow{C_2}.\overrightarrow{U_2}) + (\overrightarrow{C_3}.\overrightarrow{U_3} - \overrightarrow{C_4}.\overrightarrow{U_4})] \tag{5}$$

In Equation 5, 'ρ' is the density of the fluid (water); 'Q', flow rate; and 'P', power [13].
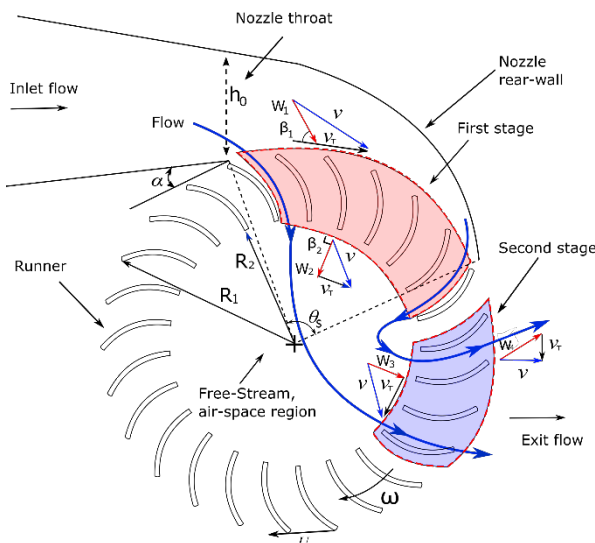

Fig. 10. Velocity triangle in the runner of the Michell-Banki turbine [19].

The pressure contours in Fig. 11 represent each turbine model under study. Profile 20-32C causes a higher pressure at the nozzle inlet than the other models, all under the same simulation conditions. This pressure increase can be associated with a higher fluid velocity inside the nozzle, which causes a greater transformation of potential energy into kinetic energy at the runner inlet. For this reason, the turbine configured with this blade profile achieves the best efficiency.
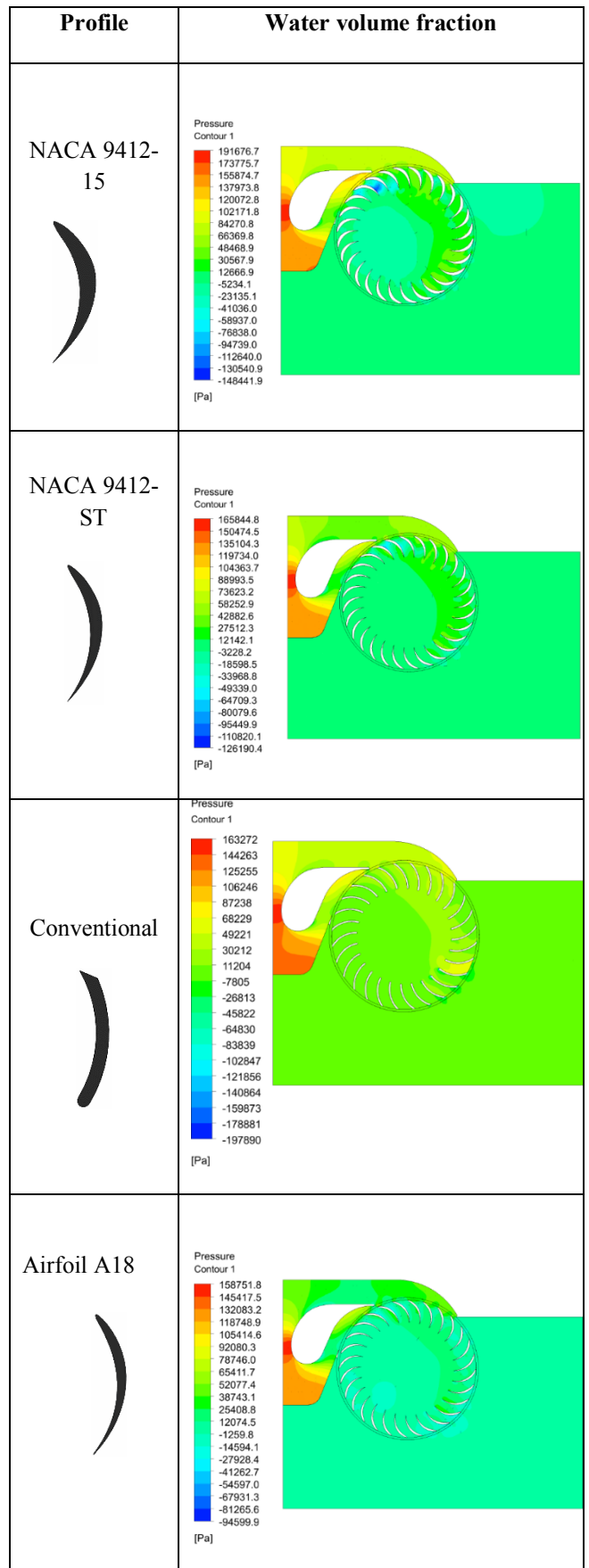
Profile	Water volume fraction
20-32C	

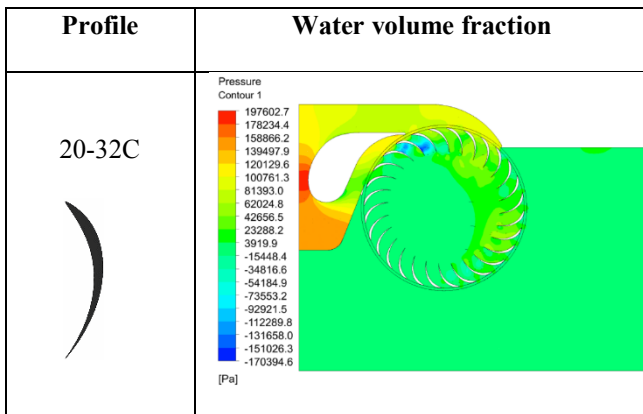| Profile	Water volume fraction
NACA 9412-15	
NACA 9412-ST	
Conventional	
Airfoil A18	

Fig. 11. Pressure contours of each turbine model.

4. **Conclusions**

The incidence of the blade profile on the efficiency of the runner of a Michell Banki Cross-Flow turbine was numerically validated with CFD simulation of five turbine models in ANSYS CFX® V 18.1. Four of them were fitted with hydrodynamic profiles 20-32C, A18, NACA 9412-15 and NACA 9412-ST; the other one was the reference model with a tube-type conventional blade profile. The turbine configured with the 20-32C profile achieved a 90.6% efficiency, i.e. a 7.37% increase over a conventional blade turbine.

ANSYS CFX® is a very useful simulation tool for this type of research related to fluid dynamics, since the resulting simulation data are reliable. Hence, building a model of a Michell Banki turbine configured with the 20-32C profile and conducting experiments under the same operating conditions in this study could show the extent to which the experimental results match this numerical simulation.

The literature contains several studies that aim to improve the efficiency of a turbine based on its geometric parameters, but they do not focus on the profile of the blades. However, this work demonstrates that such feature has an important influence on the efficiency of the Michell Banki turbine.

Acknowledgements

References

[1]   P. Lojano, J. Cabrera, A. Lojano, D. Morales, and D. Icaza, "Voltage data collection using arduino and matlab of a photovoltaic wind power system in the locality of tarqui the cuenca ecuador," in *8th International Conference on Renewable Energy Research and Applications*, 2019, pp. 582–586, doi: 10.1109/ICRERA47325.2019.8997035.

[2]   M. R. D. and D. S. C., "CFD Study of a Vertical Axis Counter-Rotating Wind Turbine," in *6th International Conference on Renewable Energy Research and Applications*, 2017, vol. 5, doi: 10.1109/ICRERA.2017.8191273.

[3]   D. Icaza and D. Borge-Diez, "Potential sources of renewable energy for the energy supply in the city of cuenca-ecuador with towards a smart grid," in *8th International Conference on Renewable Energy Research and Applications*, 2019, pp. 603–610, doi: 10.1109/ICRERA47325.2019.8997114.

[4]   D. S. Semerci and T. Yavuz, "Increasing efficiency of an existing francis turbine by rehabilitation process," in *International Conference on Renewable Energy Research and Applications*, 2016, vol. 5, pp. 107–111, doi: 10.1109/ICRERA.2016.7884440.

[5]   N. Unidas, "La sostenibilidad del desarrollo a 20 años de la cumbre de la tierra: Avances, brechas y lineamientos estratégicos para América Latina y el Caribe," 2011.

[6]   D. Andrade, C. Curiel, F. Kenyery, O. Aguill, and M. Asuaje, "Numerical Investigation of the Internal Flow in a Banki Turbine," *Int. J. Rotating Mach.*, pp. 1–12, 2011, doi: 10.1155/2011/841214.

[7]   Ossberger, "La turbina original OSSBERGER ® de flujo cruzado," Weißenburg/Alemania, 2016.

[8]   J. Zanette, D. Imbault, and A. Tourabi, "A design methodology for cross flow water turbines," *Renew. Energy*, vol. 35, no. 5, pp. 997–1009, 2010, doi: 10.1016/j.renene.2009.09.014.

[9]   D. Adanta, A. I. Siswantara, and A. P. Prakoso, "Performance Comparison of NACA 6509 and 6712 on Pico Hydro Type Cross- Flow Turbine by Numerical Method," *J. Adv. Res. Fluid Mech. Therm. Sci.*, no. May, 2018.

[10]   L. i. V. garcía and W. M. E. Monsalve, "Análisis de la Influencia del Porcentaje de Apertura del Alabe Director Sobre la Potencia Hidráulica de un Pico Generador de Flujo Cruzado Mediante un Estudio Numérico en Software CFD," Universidad de antioquia, 2012.

[11]   V. Sammartano, C. Aricò, A. Carravetta, O. Fecarotta, and T. Tucciarelli, "Banki-Michell optimal design by computational fluid dynamics testing and hydrodynamic analysis," *Energies*, vol. 6, no. 5, pp. 2362–2385, 2013, doi: 10.3390/en6052362.

[12]   "A numerical investigation of flow profile and performance of a low cost Crossflow turbine," *Int. J. Energy Environ.*, vol. 5, no. 3, pp. 275–296, 2014.

[13]   Y. C. Ceballos, M. C. Valencia, D. H. Zuluaga, J. S. Del Rio, and S. V. García, "Influence of the number of blades in the power generated by a Michell Banki Turbine," *Int. J. Renew. Energy Res.*, vol. 7, no. 4, pp. 1989–1997, 2017.

[14]   Mario Alfonso Arellano Vilchez, "Geometría del álabe del rotor para mejorar el toruqe en una turbina Michell-Banki," 2015.

[15]   C. A. H. Bazo, "Diseño y Estandarización de Turbinas Michell-Banki," *Organ. Latinoam. Energía*, p. Quito-Ecuador, 1980.

[16]   A. Benzerdjeb, B. Abed, H. Achache, M. K. Hamidou, M. Bordjane, and A. M. Gorlov, "Numerical study on the performance of darrieus turbine by K-ϵ standard and K-ϵ EARSM turbulence models," in *2017 6th International Conference on Renewable Energy*

Research and Applications, 2017, pp. 528–533, doi: 10.1109/DISTRA.2017.8191117.

[17]   I. ANSYS, "ANSYS CFX-Solver Theory Guide," *release*. U.S.A, 2013.

[18]   C. A. Mockmore and F. Merryfield, "The Banki Water Turbine, Engineering Experiment Station (of Oregon State College)," *Bull. Ser.*, no. 25, p. 2, 1949.

[19]   R. C. Adhikari and D. H. Wood, "A new nozzle design methodology for high efficiency crossflow hydro turbines," *Energy Sustain. Dev.*, vol. 41, pp. 139–148, 2017, doi: 10.1016/j.esd.2017.09.004.